Proceedings of ASME Turbo Expo 2020
Turbomachinery Technical Conference and Exposition
GT2020
June 22-26, 2020, London, England

GT2020-15495

OPTIMIZATION OF LARGE OFFSHORE WIND FARM LAYOUT CONSIDERING RELIABILITY AND WAKE EFFECT

Xiangyu Li[1], Cuong D. Dao, Behzad Kazemtabrizi, and Christopher J. Crabtree

[1]Department of Engineering, Durham University, South Road, Durham, DH1 3LE, UK

ABSTRACT

Nowadays, the increasing demand of electricity and environmental hazards of the greenhouse gas lead to the requirement of renewable energies. The wind energy has been proved as one of the most successful sustainable energies. Recently, the development trend of the wind energy is to build large offshore wind farms (OWFs) with hundreds of wind turbines, which could generates more power in one wind farm. In the large OWF, the wake effect is a very important impact factor to the wind farms, especially for those with close spacing. Therefore, the wind farm layout, the location of the wind turbines (WTs) is very essential to the performance of the whole wind farm, especially for large OWFs. In this research, we focus on the optimization of the large OWF layout by considering performance of the OWF, such as the total output energy. Firstly, the model for wind farm performance evaluation is established by incorporating historical wind speed data and the wake effect which can affect the total wind farm output. Then, by using the metaheuristic algorithms, the genetic algorithm(GA), the OWF layout is optimized. This study can offer useful information to the wind farm manufactures in the large OWF design phase.

NOMENCLATURE

(x_i, y_i)	The coordinate of the WTs
P_{WF}	The output power of the wind farm
v_0	Approaching wind speed
v_d	Wind speed for the downstream WT
R_0	Diameter of the WT rotor
A_S	The shade area of the wake effect
A_{WT}	Swept area of the WT
C_t	WT thrust coefficient
α_{wake}	The wake expansion rate
λ_i, u_i	The failure and repair rate of subassembly i
λ_{WT}, u_{WT}	The failure and repair rate of WT
Ava_{WT}	The availability of the WT

1. INTRODUCTION

Nowadays, the demand for sustainable energy grows rapidly and the offshore wind farms consisted of multiple-wind turbines (WT) can generate a lot of powers [1]. The offshore wind is becoming more and more important as newly developed technology has enabled the installation of multi-megawatt scale wind turbines (WTs) suitable for far offshore locations [2]. And the development trend of the offshore wind energy is to build large offshore wind farms with hundreds of wind turbines, which could generates more power within one wind farm.

In the wind farm, the WTs generate power by the wind, and according to the energy conservation principle, the wind speed entering a WT is higher than leaving it. As a result, the WTs located behind other WTs will face a lower wind speed and generate less power, called the wake effect loss. The wake effect in the wind farms can lead to obvious power losses, high up to 50% in some wind farms due to the close spacing [3]. Generally, the wake effect is highly related to the wind farm layout, i.e., relative distance and angle among the WTs. On the other hand, the WT reliability also has a great impact on the wind farm output [4]. Therefore, in this paper, we focus on the wind farm layout optimization to minimize the wake losses considering the wake effect and WT reliability.

In the literature, many researchers have proposed many methods to optimize the wind farm layout to maximize the output power or minimize the cost. Most of these researches are focused on reducing the initial investment, which can be transferred into minimizing the total connection AC cable length/cable cost. To deal with this problem, Ouahid proposed a method to represent different connection topologies by the adjacent matrix, and the GA is used to solve this NP-hard optimization problem [5]. Then,

[1] Contact author: xiangyu.li@durham.ac.uk

Ouahid applied this method in optimizing the offshore wind farm by considering different types of cables and using the OWF called 'Banc de Guérande' as a practical example [2]. After this, Ouahid used the same OWF as practical example to explore the impact of the system reliability and different system architecture (two different connection ways and with or without the round connected cable) on the OWF reliability [6]. Sudipta proposed a method by using the external splice locations to optimize the wind farm collector system topology [7]. In [7], two k-clustered methods were introduced, by wind turbine locations and radial angles (better one), respectively. Shin improved the k-clustering method with the angle criterion [8]. By using the crossover and mutation operators from the GA, the WTs in the adjacent groups can move to other groups. And an example OWF with 80 3WM WTs showed that this improved method is better than only using GA or only using K-clustering method. Hou proposed a APSO-MST method by combining adaptive PSO and the MST method to minimize the wind farm cable cost [9]. Fischetti used the mixed-integer Linear Programming (MILP) method to minimize the cable layout cost by considering the power losses [10]. Chen proposed a self-adaptive allocation method to allocate the connection topologies and a MINLP as well as benders decomposition algorithm is adopted to minimize the cost (investment cost, maintenance cost and cable loss cost)[11]. Zuo used a self-tracking minimal spanning tree (MST) method combined with cable crossing avoiding to build the optimal wind farm layout topology to minimize the initial cable cost [12]. On the other hand, some researchers are also studied the optimization of the wind farm layout considering other impact factors. Wu used the charged system search (CSS) optimization algorithm to optimize the WT layout positions [13]. And the Wind Atlas Analysis and Application Program software is used to verify the result. Banzo used stochastic optimization method to optimize the wind farm design considering three impact factors: investments, system efficiency and system reliability[14]. Ahmad used the turbulence intensity–based Jensen model TI-JM to describe the wake effect and optimized the yaw-offset to maximize the wind farm output by particle swarm optimization (PSO) [3].

All these methods mentioned above have an assumption that all the WT positions are fixed. In the traditional design of the wind farm, the WTs are always constructed in lines. In this kind of layout, the wake effect is very strong in some wind directions, such as the wind direction paralleled with the WT line. Therefore, we focus on this problem, and by using the Jensen wake effect model and improved GA, an optimization procedure for minimizing the wake effect is proposed.

The rest of this paper is organized as follows. Section 2 introduces the optimization problem and its formulation. The Jensen model and the rotating coordinating system are introduced detailed in section 3. In addition, the 2-state Markov model for components and WT reliability evaluation are also presented. Then, an optimization procedure based on an improved GA is shown in section 4. A case study with 8 5-MW WTs is used to illustrate the presented methods in section 5. Section 6 gives the conclusions and future works.

2. OPTIMIZATION PROBLEM

In this section, we shall define the variables and assumptions on the wind farm layout. And the mathematical formulation of the optimization problem is also introduced.

The objective of this optimization is to find the optimal layout of the wind farm, i.e., the positions of all the WTs to minimize the wake effect loss. So the optimization variables are the coordinates (x_i, y_i) of all the WTs in the wind farm.

The optimization of the wind farm layout is a very complex problem, so there are some assumptions are made,

(1) All the WTs are connected by the AC cables and the failures of AC cables are not considered, which means that all the electricity generated by the WTs are transited to the onshore station;

(2) The numbers of the WTs are fixed.

In this research, the objective of this optimization is to minimize the wake losses, on another word, maximize the output energy. Therefore, the optimization problem can be formulated as,

$$\begin{aligned} \max \quad & P_{WF} = \sum_{i=1}^{n} f\left((x_i, y_i), (v_{wind}, \alpha_{wind}), (\lambda_j^c, u_j^c), \alpha_{wake}\right) \\ s.t. \quad & \begin{cases} x_i \in [x_{i,\min}, x_{i,\max}] \\ y_i \in [y_{i,\min}, y_{i,\max}] \end{cases}, \quad i \in [1, 2, \cdots, n] \end{aligned} \tag{1}$$

where n is the number of the WTs in the wind farm. v_{wind} and α_{wind} are the free wind speed and wind direction. λ_j^c and u_j^c are the failure and repair rates of the jth component in WTs. α_{wake} is the wake expansion rate. Eq. (1) give the constraints that all the WTs can only change their positions in a constraint area, so the positions of the WTs do not overlap with each other.

3. WIND FARM PERFORMANCE EVALUATION CONSIDERING RELIABILITY AND WAKE EFFECT

3.1 Wake effect model

In a wind farm, according to the momentum conservation, the wind velocity will decrease after the blowing the blades of the WT, which results in wake effects. In practice, the power losses can be as high as 50% in some wind farms with close spacing. In recent years, many wake models have been proposed to describe the wake effect. In this paper, the most commonly used Jensen model is used to explain the wake effect of the wake effect among WTs [3]. In the Jensen model, the wake effect is assumed to be expanded linearly and only depends on the between WTs and wind directions, as shown in Figure 1.

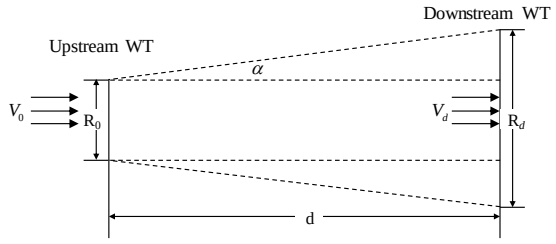

Figure 1: JENSEN MODEL PRINCIPLE.

By using the Jensen model, the wind speed for all the downstream WTs can be evaluated as,

$$v_d = v_0\left(1-\left(1-\sqrt{C_t}\right)\left(\frac{R_0}{R_0+2\alpha_{wake}d}\right)^2\right) \quad (2)$$

where v_0 is the approaching or free wind speed, C_t is the WT thrust coefficient, R_0 is the WT diameter, α_{wake} is the wake expansion rate, and d is the downstream distance.

Moreover, the wind turbine can also be affected by the neighbor turbines, which means that may only part of the WT lies in the wake effect area, called the wind shade effect. By considering the wake shade effect, Eq. (2) can be modified as,

$$v_d = v_0\left(1-\left(1-\sqrt{C_t}\right)\left(\frac{R_0}{R_0+2\alpha_{wake}d}\right)^2\left(\frac{A_S}{A_{WT}}\right)\right) \quad (3)$$

where A_S is the shadow area by other WTs, shown as the Figure 2 and A_{WT} is the swept area of the downstream WT. In Figure 2, r_1 and r_0 are the radius of the wake area at distance d and the WT, respectively. And Y is the distance between two centers. The shadow area of the downstream WT could change along with the change of the wind speed direction.

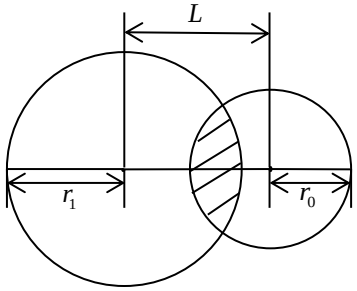

Figure 2: THE WAKE SHADOW EFFECT.

According to the value of A_s / A_{WT}, the wake effect can be divided into three categories:

- $A_s / A_{WT} = 0$, there is no wake effect for the target WT.
- $A_s / A_{WT} = 1$, the whole target WT lies in the wake effect area.
- $0 < A_s / A_{WT} < 1$, only part of the WT lies in the wake effect area.

For $0 < A_s / A_{WT} < 1$, the shadow area A_s, as shown in Figure 2, can be evaluated as,

$$A_s = r_1^2 \arccos\left(\frac{r1^2+L^2-r0^2}{2Lr_1}\right)+r_0^2\arccos\left(\frac{r1^2+L^2-r1^2}{2Lr_0}\right) - Lr_1\sin\left(\arccos\left(\frac{r1^2+L^2-r0^2}{2Lr_1}\right)\right) \quad (4)$$

A wind turbine may be affected by wakes from multiple upstream WTs, so the cumulated wake effect should be considered. Therefore, Eq. (3) can be further derived as,

$$v_d = v_0\left(1-\sum_{i=1}^{n}\left(1-\sqrt{C_t}\right)\left(\frac{R_0}{R_0+2\alpha_{wake}d_i}\right)^2\left(\frac{A_{Si}}{A_{WT}}\right)\right) \quad (5)$$

Where n is the number of the upstream WTs of the target wind turbines, d_i and A_{Si} are the distance and shadow area of the ith upstream WT on the target WT.

By the Jensen multiple wake effect model, the wind speed for each downstream WT can be evaluated.

3.2 Rotating coordinate system

It is assumed that by the control of the yaw system, the WTs are always face the wind direction. So the downstream WTs and the shadow areas will changes along with the wind directions, shown as Figure 3. To evaluate the wake effect under different wind directions, the WT coordinates system is constructed along with the change of wind direction. The WT coordinates construction process is shown as follows:

Step 1, construct the original coordinate system of the wind farm with a coordinate origin (x_0, y_0). Then, the original coordinate of each WT, (x_0^i, y_0^i), can be determined, shown as Figure 3.

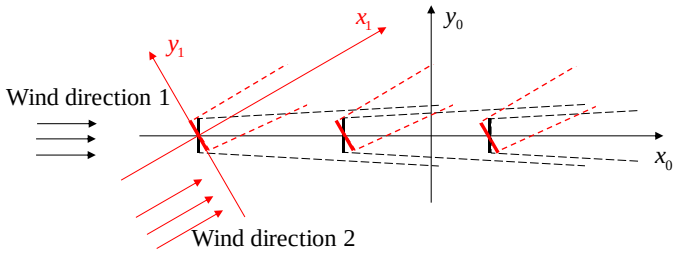

Figure 3: ROTATE COORDINATE SYSTEM

Step 2, construct the new coordinate system for each wind direction. Using wind direction 2 in Figure 3 as an example, taking the WT that experiences the wind firstly as the new origin point, the new coordinate system for this wind direction can be constructed, shown as the (x_1, y_1). Assuming the angle of wind direction 2 is θ, the coordinates of other turbines can be evaluated as,

$$x_1^i = \left(x_0^i - x_0^1\right)\cos\theta + \left(y_0^i - y_0^1\right)\sin\theta$$
$$y_1^i = -\left(x_0^i - x_0^1\right)\sin\theta + \left(y_0^i - y_0^1\right)\cos\theta \quad (6)$$

Step 3, evaluate wind speed for each WT according to the wind direction and Jensen model in the last section. Then, by repeating steps 2 and 3, the wake effect for all directions can be evaluated.

3.3 POWER CURVE

In this paper, the power generated by the WT, $P_0(t)$, is evaluated by a classical WT wind power curve [4], shown as follows,

$$P_0(t)=\begin{cases}0, & 0\le v_t<v_{cut-in}\\ \frac{1}{2}\rho C_p A_{WT} v_t^3, & v_{cut-in}\le v_t<v_{rated}\\ P_{rated}, & v_{rated}\le v_t\le v_{cut-out}\\ 0, & v_t>v_{cut-out}\end{cases} \quad (7)$$

where C_p is the power coefficient, ρ is the air density, A_{WT} is the WT swept area, P_{rated} is the WT rated power and these three values are assumed fixed. v_{cut-in}, v_{rated} and $v_{cut-out}$ are the WT cut-in, rated and cut-out speed, respectively. By the wind power curve and wind speed for each turbine, the wind power generated by each WT under different wind speed and direction can be evaluated.

3.4. RELIABIILTY MODEL

In the last section, the power generated under different wind speed and directions are evaluated, but that is under assumption that the WT doesn't fail. Al the components in the WTs may degraded into failure state. So the reliability of the WT is also considered in the power generation.

The WTs are consisted of several components and subsystems, such as blades, drivetrain, generator, pitch, etc. In this paper, the PMSG DD WT is studied, which is a proper type for the large OWFs. In the PMSG DD WT, if any component fails, the whole WT will stop working, so all the components are connected in series logically.

Assuming that the failure and repair time follow the exponential distribution with parameter λ_i and u_i. Then, the degradation process of the components can be regarded as a 2-state Markov process. All the components are connected in series, so the WT can be also regarded as a 2-state Markov process, shown as Figure 4.

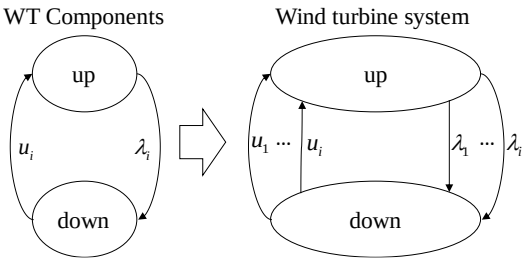

Figure 4: RELIABILITY MODEL FOR WT COMPONENTS AND WT SYSTEM.

According to the Markov process, the failure rate and repair rate of the WT, λ_{WT} and u_{WT}, can be evaluated with the components' failure parameters, shown as,

$$\lambda_{WT}=\sum_{i=1}^{n}\lambda_i,\qquad u_{WT}=\sum_{i=1}^{n}\lambda_i/\sum_{i=1}^{n}(\lambda_i/u_i) \quad (8)$$

In Eq. (8), n is the number of the WT components. Then, the availability of the WT, Ava_{WT}, can be evaluated as,

$$Ava_{WT}=\left(1+\sum_{i=1}^{n}\lambda_i/u_i\right)^{-1} \quad (9)$$

By incorporated the reliability of the WT system, the power curve equation with considering the WT reliability, $P_0^R(t)$, can be derived as,

$$P_0^R(t)=\begin{cases}0, & 0\le v_t<v_{cut-in}\\ \frac{1}{2}\rho C_p A_s v_t^3\cdot Ava_{WT}, & v_{cut-in}\le v_t<v_{rated}\\ P_{rated}\cdot Ava_{WT}, & v_{rated}\le v_t\le v_{cut-out}\\ 0, & v_t>v_{cut-out}\end{cases} \quad (10)$$

By Eq. (10) and the wind speed by the wake effect model, the total energy output of one wind farm under specific wind speed and wind direction can be evaluated, which is also be used as the objective function in the following optimization part.

4. OPITIMISATION TECHNOLOGY

Assuming that there are n turbines in one wind farm and the possible positions for each turbine is $n_x\times n_y$. (n_x,n_y) are possible coordinates. Then, the maximum of possible position combination for all WTs is $n^{n_x\times n_y}$. It is very difficult and time consuming to evaluate them one by one. Therefore, the GA, a commonly used optimization technique, is applied to optimize the wind farm layout.

The GA is a method inspired by the biological genetics. In the GA, each solution is coded as binary variables, called the 'chromosomal'. Then, by imitating the genetic evolutionary process, a group of the solutions are optimized step by step by using the crossover, mutation and selection procedures. During the optimization process, the best individual of each generation is kept and passed directly to the next generation, called the elite strategy.

The optimization procedure is shown as follows and Figure 5.

(1) Initiation: ascertain the population number (N_A), the max iterations ($N_{\max}$) and the restrictions. Then, construct the chromosomal according the encoding rules.

(2) Generate initial population randomly, and the output power for each individual can be evaluated by the evaluation procedure introduced above. Then evaluate the fitness for each individual.

(3) If the iterations $n<N_{\max}$, continue to optimize the chromosomal by crossover, mutation and selection procedures, then set $n=n+1$;

(4) Terminating condition: The number of iteration $n=N_{\max}$, otherwise the optimization procedure goes back to step (3).

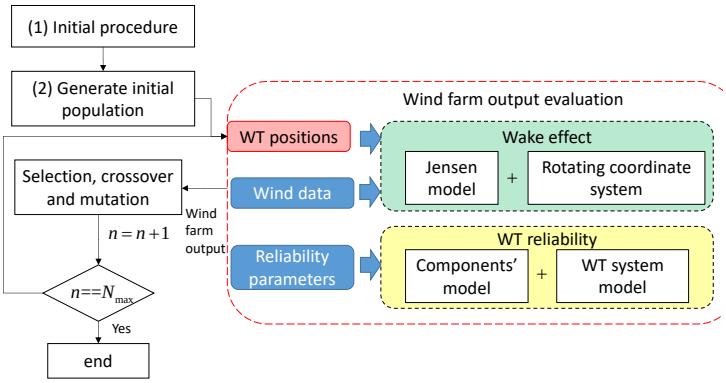

Figure 5: THE OPTIMIZATION PROCEDURE.

5. CASE STUDY

5.1. WIND FARM CASE

Consider one wind farm with eight 5-MW WTs and the area for the WTs are shown in Figure 6. Traditionally, the WTs are always arranged in lines. Therefore, the first benchmark layout of this wind farm is shown as Figure 6(a) and D is rotor diameter. The wake effect for the wind direction from the wind direction 180° is also shown in Figure 6(a). In some cases, the WTs are also misaligned of half spacing to increase the relative distances to reduce the wake effect. This kind of layout is used as another benchmark case, shown as Figure 6(b).

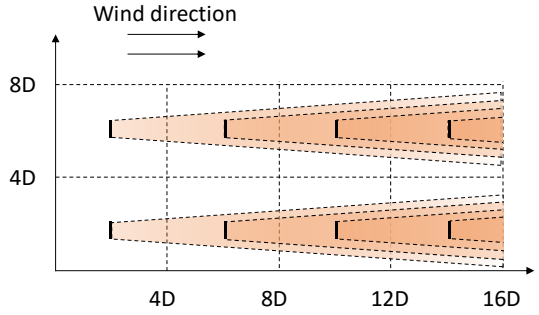

(a) Benchmark layout A

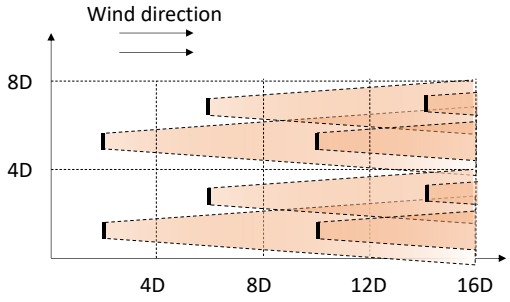

(a) Benchmark layout B

Figure 6: WT POSITIONS AND WAKE EFFECT OF THE BENCHMARK CASES.

The range of each WT is also shown in Figure 6 and listed in Table 1.

Table 1. WIND TURBINE SPECIFICATION

Parameter	Range of x coordinate	Range of y coordinate
WT 1	[0, 4*D]	[0, 4*D]
WT 2	[4*D,8*D]	[0, 4*D]
WT 3	[8*D, 12*D]	[0, 4*D]
WT 4	[12*D, 16*D]	[0, 4*D]
WT 5	[0, 4*D]	[4*D, 8*D]
WT 6	[4*D,8*D]	[4*D, 8*D]
WT 7	[8*D, 12*D]	[4*D, 8*D]
WT 8	[12*D, 16*D]	[4*D, 8*D]

The parameters of the exemplar WT is coming from [16] and presented in Table 2.

Table 2. WIND TURBINE SPECIFICATION

Parameter	Value
Power rating (MW)	5
Rotor diameter (m)	126
Cut-in wind speed (m/s)	3
Rated wind speed (m/s)	11.4
Cut-out wind speed (m/s)	25
Power factor (C_p)	0.44
wake expansion rate α_{wake}	0.05

On the other hand, six major components, Blades, Pitch, Drivetrain, Generator, Convertor, and Other Electricals are considered in the reliability modeling. And the failure rates and repair hours of all the components are extracted from [4], shown in Table 3.

Table 3. INPUT RELIABILITY DATA

Component	Failure rate (per WT per year)	Downtime per failure (hours)
Blades	0.1723	99.35
Pitch	0.1175	51.22
Drivetrain	0.0239	156.85
Generator	0.1189	179.34
Converter	0.1222	66.54
Other electrical	0.2815	52.48

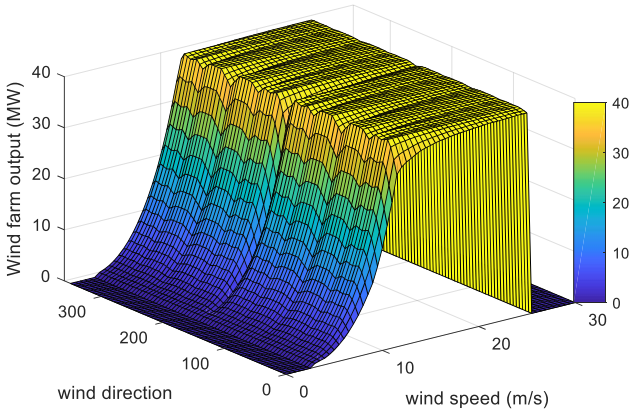

Figure 7: OUTPUT POWER CURVE OF THE WIND FARM UNDER DIFFERENT WIND DIRECTION.

Then, by the models proposed in previous sections, the output power curve for this wind farm under different wind directions are shown in Figure 7. From Figure 7, we can see that the wake losses are very obvious in some directions. So to minimize the wake effect, we need to evaluate the output energy by considering both the wind speed and direction data.

To extract the wind speed data, the Lillgrund wind farm [3], located in Denmark is chosen as an example, and 10 years historical wind speed and direction data at this place is downloaded from [17]. And the wind rose graph for this data set is also shown in Figure 8.

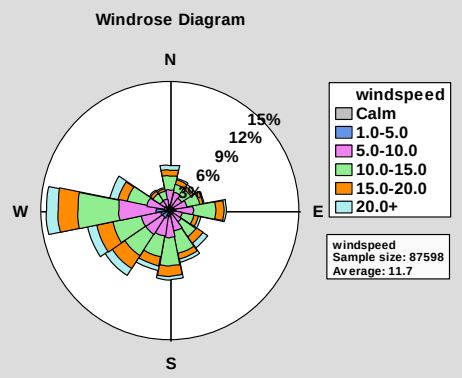

Figure 8: THE WIND ROSE MAP OF THE WIND DATA SET.

By the this wind data set, the total energy output of this wind farm with benchmark design is $P_{WF,Be1} = 2.0531\times10^{6} MWh$ $P_{WF,Be2} = 2.0989\times10^{6} MWh$.

Then, by the optimization procedure shown in section 4 and the basic GA parameters shown in Table 4, the optimization result is shown in Figure 9. From Figure 9, we can see that the algorithm reaches to the optimal solution at about 200 generations and the best result varies very slightly in the remaining iterations.

Table 4. THE GA OPTIMIZATION PARAMETER.

Parameters	Value
Max iteration	500
Mutation rate	0.1
Population	30
GGAP	0.9
Crossover	0.7

The optimal layout is shown in Figure 10 and the accurate positions of the WTs are also listed in Table 5. The energy output with the WT positions listed in Table 5 is $P_{WF,OP} = 2.1549\times10^{6} MWh$. Compared to the benchmark layout structure, the total output by the optimal wind farm layout design increases by 4.96 and 2.67 percent compared to benchmark layouts A and B, respectively.

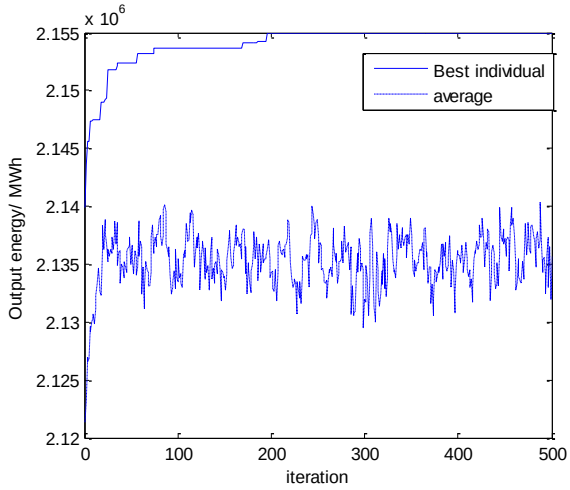

Figure 9: EVALUATION OF THE BEST AND AVERAGE FITNESS OF EACH GENERATION.

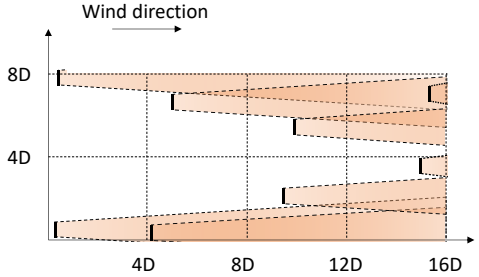

Figure 10: EVALUATION OF THE BEST AND AVERAGE FITNESS OF EACH GENERATION

Table 5. THE ACCURATE POSITIONS OF THE WTS AFTER OPTIMIZATION.

	Coordinate
WT 1	(0, 1.8*D)
WT 2	(4.8*D, 0.4*D)
WT 3	(9.1*D, 0*D)
WT 4	(15.8*D, 0.1*D)
WT 5	(0.4*D, 7.8*D)
WT 6	(4.4*D, 8.0*D)
WT 7	(10.2*D, 7.9*D)
WT 8	(15.1*D, 6.5*D)

5.2. ROBUST ANALYSIS

In this section, to analysis the robust of the proposed method, the various input reliability data is used as an example. The failure rate and repair rate of each component is set to vary from 50% to 150% of the input data and the optimal output energy is shown as Figure 11.

From Figure 11, an expected trend that the optimal output energy decreases as the failure rate increases or the repair rate decreases is observed, which can verified the robust of this method.

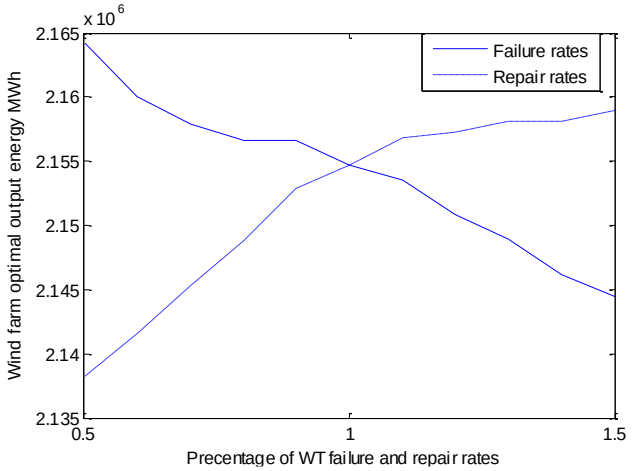

Figure 11: RUBUST ANALYSIS OF THE METHOD BY DIFFERENT IPUT RELIABILITY DATA

6. CONCLUSIONS

This paper present a layout optimization procedure for a multi-megawatt DD offshore wind farm considering both WT reliability and wake effect among WTs. By using Jensen model and rotating coordinate system, the wind farm output curve can be generated. And by the Markov model, the reliability of the WTs is also considered in the output power evaluation. By using the evaluated output power as objective, the layout of the wind farm is optimized by an improved GA. The results show that:

(1) The output of the wind farm is sensitive to the wind direction due to the wake effect;

(2) By moving the positions of the WTs, the wake losses can be reduced. In the case study, the output is increased by up to 4.96%.

In the future research works, the reliability of other parts of the wind farm, such as cables, offshore stations will be considered as impact factors also. And the optimization of the connection topology between the WTs in the wind farm is another research issue.

ACKNOWLEDGEMENTS

This work is supported by the UK Engineering and Physical Sciences Research Council (EPSRC) HOME-Offshore project (EPSRC Reference: EP/P009743/1).

REFERENCES

[1]. Sayas F C, Allan R N. Generation availability assessment of wind farms[J]. IEE Proceedings-Generation, Transmission and Distribution, 1996, 143(5): 507-518.

[2]. Dahmani O, Bourguet S, Machmoum M, et al. Optimization of the connection topology of an offshore wind farm network[J]. IEEE Systems Journal, 2014, 9(4): 1519-1528.

[3]. Ahmad T, Basit A, Anwar J, et al. Fast Processing Intelligent Wind Farm Controller for Production Maximisation[J]. Energies, 2019, 12(3): 544.

[4]. C. D. Dao, B. Kazemtabrizi, and C. J. Crabtree, "Modelling the Effects of Reliability and Maintenance on Levelised Cost of Wind Energy," the ASME 2019 Turbo Expo, Phoenix, Azirona, USA, 2019.

[5]. Dahmani O, Bourguet S, Guerin P, et al. Optimization of the internal grid of an offshore wind farm using Genetic Algorithm[C]//2013 IEEE Grenoble Conference. IEEE, 2013: 1-6.

[6]. Dahmani O, Bourguet S, Machmoum M, et al. Optimization and reliability evaluation of an offshore wind farm architecture[J]. IEEE Transactions on Sustainable Energy, 2016, 8(2): 542-550.

[7]. Dutta S, Overbye T J. Optimal wind farm collector system topology design considering total trenching length[J]. IEEE Transactions on Sustainable Energy, 2012, 3(3): 339-348.

[8]. Shin J S, Kim J O. Optimal design for offshore wind farm considering inner grid layout and offshore substation location[J]. IEEE Transactions on Power Systems, 2016, 32(3): 2041-2048.

[9]. Hou P, Hu W, Chen Z. Optimization for offshore wind farm cable connection layout using adaptive particle swarm optimization minimum spanning tree method[J]. IET Renewable Power Generation, 2016, 10(5): 694-702.

[10]. Fischetti M, Pisinger D. Optimizing wind farm cable routing considering power losses[J]. European Journal of Operational Research, 2018, 270(3): 917-930.

[11]. Chen Y, Dong Z Y, Meng K, et al. Collector system layout optimization framework for large-scale offshore wind farms[J]. IEEE Transactions on Sustainable Energy, 2016, 7(4): 1398-1407.

[12]. Zuo T, Meng K, Tong Z, et al. Offshore wind farm collector system layout optimization based on self-tracking minimum spanning tree[J]. International Transactions on Electrical Energy Systems, 2019, 29(2): e2729.

[13]. Wu Y K, Su P E, Su Y S, et al. Economics-and reliability-based design for an offshore wind farm[J]. IEEE Transactions on Industry Applications, 2017, 53(6): 5139-5149.

[14]. Banzo M, Ramos A. Stochastic optimization model for electric power system planning of offshore wind farms[J]. IEEE Transactions on Power Systems, 2010, 26(3): 1338-1348.

[15]. Liu Y, Zhang B, Jiang T, et al. Optimization of Multilevel Inspection Strategy for Nonrepairable Multistate Systems[J]. IEEE Transactions on Reliability, 2019.

[16]. J. Jonkman, S. Butterfield, W. Musial, and G. Scott, "Definition of a 5-MW Reference Wind Turbine for Offshore System Development," NREL/TP-500-38060, 947422, 2009.

[17]. https://mesonet.agron.iastate.edu/request/download.phtml.